ELSEVIER

Journal of Power Sources 53 (1995) 119–125

JOURNAL OF POWER SOURCES

Performance of valve-regulated lead/acid test cells for float operation using modified positive active materials

B. Szcześniak *, J. Kwaśnik, J.D. Milewski, T. Pukacka

Central Laboratory of Batteries and Cells, Poznań, Poland

Received 25 October 1994; accepted 2 November 1994

Abstract

Three types of valve-regulated lead/acid cells have been made with positive active material prepared from: (i) tribasic lead sulfate; (ii) tetrabasic lead sulfate; (iii) tetrabasic lead sulfate with graphite added. The cells have been subjected to float operation. They undergo premature capacity loss. The circumstances of this effect, the possibility of recovery of the capacity, the role of the graphite, and the impedance spectra of the cells are discussed.

Keywords: Lead/acid test cells; Valve-regulated cells; Float operation; Positive active materials

1. Introduction

The cycling performance of batteries with positive active material obtained from tetrabasic lead sulfate ($4PbO \cdot PbSO_4 = 4BS$) has been described in numerous publications. By contrast, however, information on the float operation of such batteries is scarce. Biagetti and Weeks [1] assert that results obtained from cycling duty provide a good forecast of float operation. Simon and Caulder [2] have found that positive material with a reticulate structure formed from 4BS pasted on lead–calcium grids experience considerable capacity loss during float operation.

The aim of the work presented here is to investigate whether 4BS-based material experience premature capacity loss (PCL) in valve-regulated batteries during float operation; and to evaluate the influence of graphite that is claimed [3–10] to improve the properties of positive material, especially at the beginning of battery operation.

2. Experimental

Three types of positive active material have been prepared by mixing 2 kg of leady oxide and 0.8 g of polyester fibre with 150 ml of water, and then adding 271 ml of sulfuric acid solution (1.200 sp. gr.) with further mixing. Paste 1 was obtained at room temperature. Pastes 2 and 3 were made using water heated to 80 °C. Prior to the pasting operation, the pastes were heated to 80 °C. Paste 3 contained 10 g of natural graphite RFL 1 (Kropfmöhl) with a grain size of 520 μm. All pastes were applied manually on to Pb–Ca–Sn grids (dimensions = 66.0 × 96.5 × 4.2 mm). Each plate contained 96 g of wet paste. Plates with pastes 2 and 3 were stored in a humid atmosphere at 80 °C for 72 h, while paste 1 was stored at 40 °C for 24 h. All plates were dried in air. The negative plates used the conventional paste of industrial batteries. The negative grids were 2.3 mm thick, and 45 g of wet paste was applied to each grid.

The test cells were composed of one positive plate and two negatives, separated by microglass fibre produced by Binzer with a nominal thickness of 1.4 mm. Plates of both polarities were wrapped in the separator mat. The cells were filled with sulfuric acid solution (1.200 sp. gr.) and formed. After formation, the excess electrolyte was removed. Approximately 110 g of acid remained in each cell. The test cells were equipped with safety valves and were sealed. The nominal capacity of the cell was 4.5 Ah.

The cells were subjected to float operation under constant-voltage charging at 2.25 V. Once a month, the cells were discharged at a constant current of 0.45 A to an end voltage of 1.80 V. The active material prior to formation, after formation, and then once a month was investigated by chemical analysis, X-ray diffraction (XRD) phase-analysis, and scanning electron microscopy. Impedance measurements were made in

* Corresponding author.

SSDI 0378-7753(94)02160-5

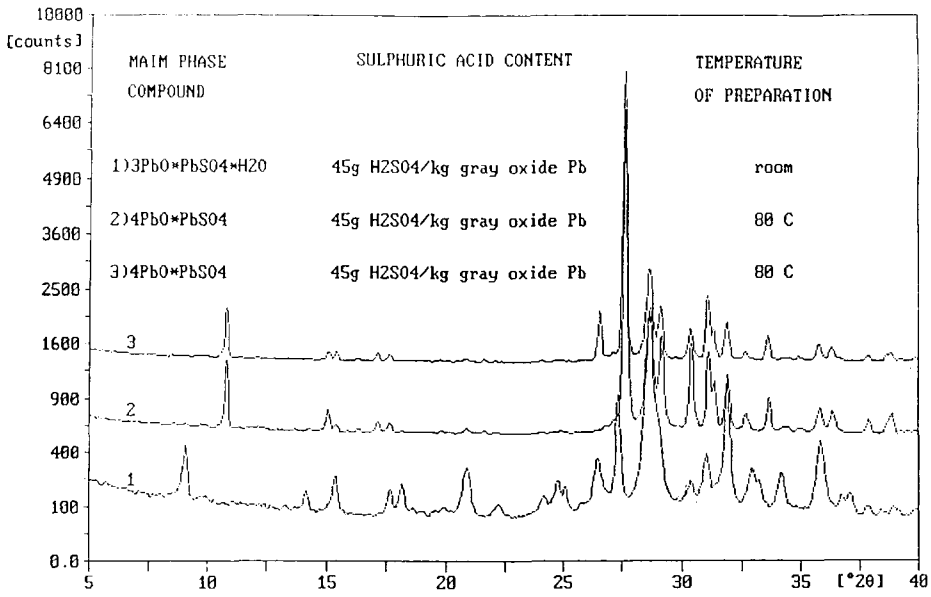

Fig. 1. X-ray diffraction patterns of positive active material before formation.

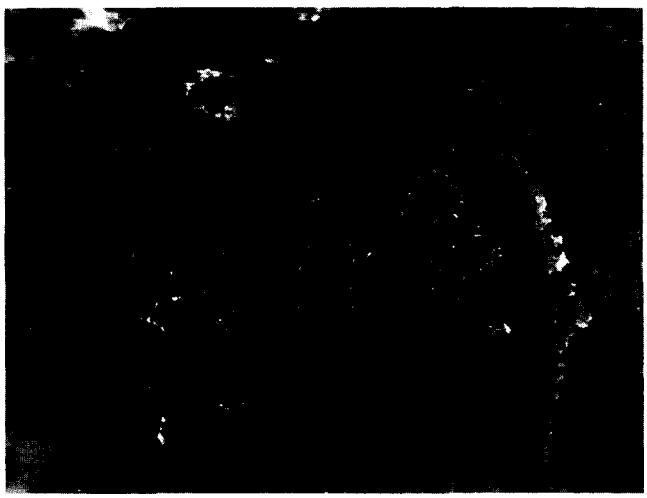

Fig. 2. Positive paste 1 before formation.

Fig. 3. Positive paste 2 before formation.

the frequency range 60–0.01 Hz using an ATLAS-91 measuring set (ATLAS-SOLLICH) and a computer with a SOFT-KAR programme.

3. Results

The XRD patterns of positive active material before formation are presented in Fig. 1. It can be seen that paste 1 contains mainly tribasic lead sulfate ($3PbO \cdot PbSO_4 \cdot H_2O = 3BS$), while pastes 2 and 3 contain 4BS. Scanning electron micrographs of the materials are shown in Figs. 2–4, respectively. A characteristic morphology is observed for the phases. Table 1 gives chemical and XRD analyses of the positive materials after formation and during float operation, at monthly intervals. Pastes 2 and 3 obtained from 4BS contain

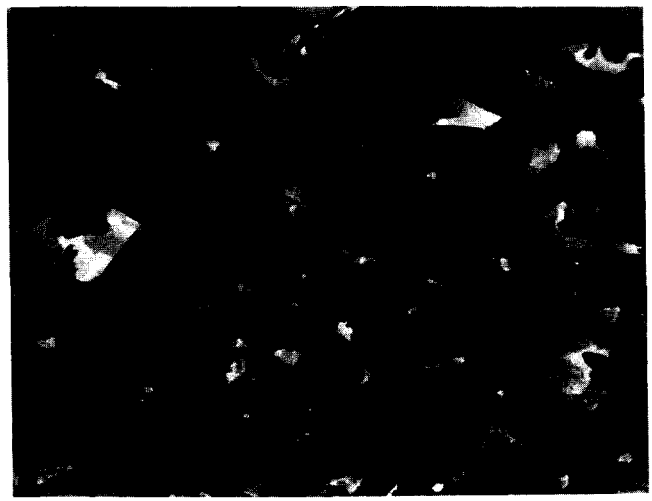

Fig. 4. Positive paste 3 before formation.

less lead dioxide just after formation than the reference paste 1 with 3BS. They also contain smaller amounts of β-PbO_2 than paste 1. The results from Table 1 are displayed graphically in Fig. 5. During float operation, the total amount of lead dioxide becomes similar for all materials, but the contents of the two crystalline phases are different. Paste 1 (3BS) contains more α-PbO_2 and less β-PbO_2 than pastes 2 and 3 (4BS). A similar α-PbO_2/β-PbO_2 is maintained during subsequent service. The morphology of these materials (shown in Figs. 6–8, respectively) also exhibits little change. Pastes 2 and 3 have a reticulate structure, while paste 1 is compact and does not transform into a coral-like structure by the end of the tests.

Table 2 gives the results of capacity measurements taken during discharge at 0.45 A after formation, and then during float operation at monthly intervals. The data are presented graphically in Fig. 9. Immediately after formation, the cell capacities are similar for all three materials. During the first month of operation, all cells experienced an increase in capacity. Cells constructed from pastes 2 and 3 exhibit a higher capacity increase than those with paste 1 obtained from 3BS. During the second month of operation, cells with paste 2 experience a slight loss in capacity, while the other cells continue to increase in capacity. During further floating, all cells suffered a decline in capacity; this was the most severe in cells with paste 2. Cells with pastes 1 and 3 were apparently better than those with paste 2 and their capacities were similar. Since the content of lead dioxide remained high all the time, it can be concluded that a part of the active material was not involved in the electrochemical reactions.

After six months of float operation, a test was performed to determine whether it is possible to recover the lost capacity. For this purpose, several cells with each material option were cycled by discharging at a

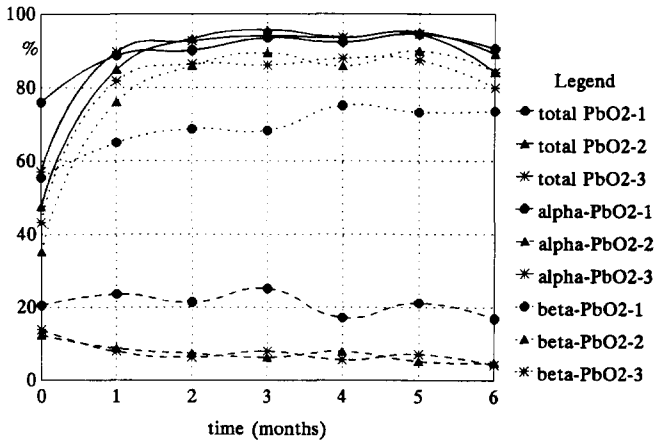

Fig. 5. Phase analysis of positive active material of experimental cells. Total PbO_2 (—): ●, paste 1; ▲, paste 2; *, paste 3. α-PbO_2 (– – –): ●, paste 1; ▲, paste 2; *, paste 3. β-PbO_2 (· · · · ·): ●, paste 1, ▲, paste 2; *, paste 3.

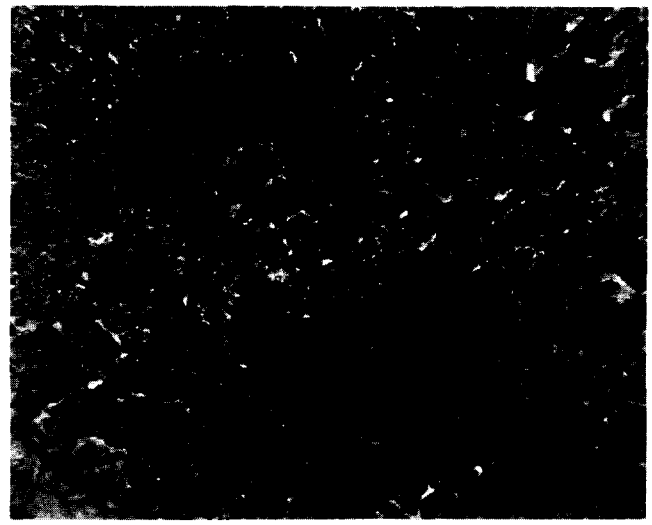

Fig. 6. Positive paste 1 after formation.

Fig. 7. Positive paste 2 after formation.

Fig. 8. Positive paste 3 after formation.

Table 1
Chemical and X-ray analyses (wt.%) of positive active material after formation and during float operation

Paste	Parameter	After formation	After 1 month	After 2 months	After 3 months	After 4 months	After 5 months	After 6 months
1	Total PbO_2	76.0	88.7	90.1	93.5	92.3	94.5	90.5
	α-PbO_2	20.5	23.6	21.4	25.1	17.2	21.2	16.9
	β-PbO_2	55.5	65.1	68.8	68.4	75.1	73.3	73.6
	$PbSO_4$	15.5	5.7	5.1	2.0	2.8	2.1	2.9
2	Total PbO_2	47.5	84.9	93.3	95.7	93.7	95.1	89.1
	α-PbO_2	12.4	8.8	7.4	6.3	7.9	5.2	4.8
	β-PbO_2	35.1	76.1	85.9	89.4	85.8	89.9	84.3
	$PbSO_4$	49.1	7.1	5.0	2.0	2.8	2.5	2.8
3	Total PbO_2	57.1	89.7	92.7	94.1	93.5	94.5	84.1
	α-PbO_2	13.9	7.9	6.3	8.0	5.6	7.1	4.2
	β-PbO_2	43.2	81.8	86.4	86.1	87.9	87.4	79.9
	$PbSO_4$	37.5	9.0	5.0	2.9	2.4	2.4	3.1

Table 2
C/10 capacity of experimental cells (Ah)

Paste	After formation	After 1 month	After 2 months	After 3 months	After 4 months	After 5 months	After 6 months	After capacity restoration procedure
1	5.3	5.9	6.4	5.5	4.4	3.0	2.5	4.4
2	5.2	7.2	6.6	4.5	2.8	1.5	1.0	1.9
3	5.2	7.3	7.4	5.8	4.4	3.1	3.5	4.3

Table 3
Phase composition (wt.%) of positive active material in failed and reactivated cells

Component	Paste 1		Paste 2		Paste 3	
	Failed	Reactivated	Failed	Reactivated	Failed	Reactivated
Total PbO_2	90.5	95.3	89.1	94.9	84.1	95.5
α-PbO_2	16.9	3.7	4.8	2.7	4.2	2.0
β-PbO_2	73.6	91.6	84.3	92.2	79.9	93.5
$PbSO_4$	2.9	2.2	2.8	2.2	3.1	2.3

low current of 0.1 A and charging at 0.45 A. The broken line in Fig. 9 represents the capacity of the 'reactivated' cells. Clearly, the cycling operation has partly improved the capacity. Cells with paste 1 almost recovered their nominal capacity. By contrast, only a partial improvement was obtained with cells using pastes 2 and 3; the effect was greater for paste 3 (with graphite) than for paste 2 (without graphite). Table 3 gives the chemical and XRD analyses of positive active material from cells 'reactivated' by cycling. There is a decrease in the α-PbO_2 content and an increase in the β-PbO_2 content.

Premature capacity loss is ascribed either to passivation phenomena at the grid/active-material interface or to changes that occur in the active material itself [11,12]. The investigations reported here suggest that

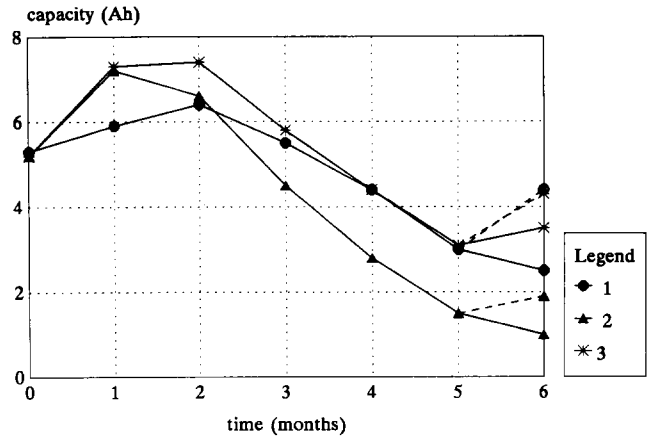

Fig. 9. Capacity of experimental cells: ●, paste 1; ▲, paste 2; *, paste 3.

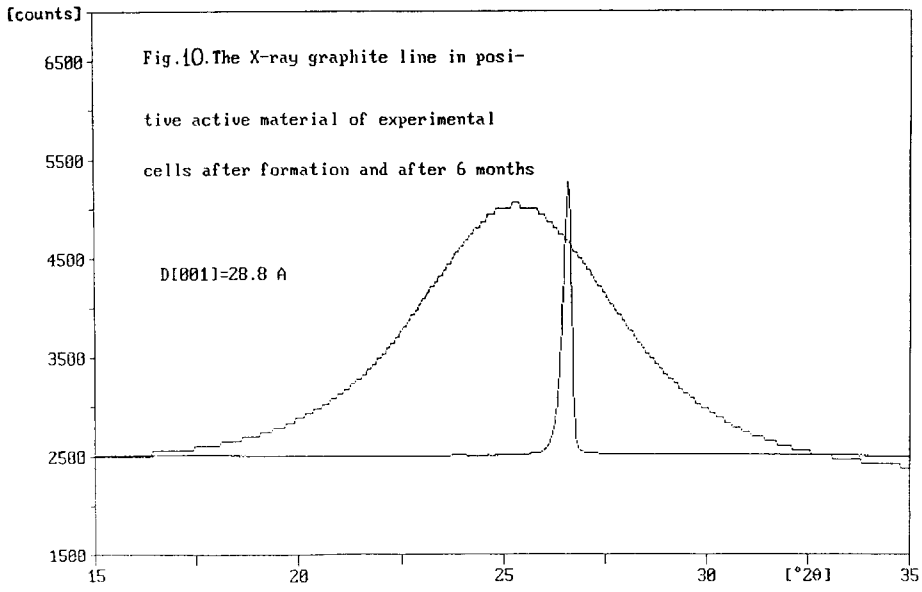

Fig. 10. X-ray line of graphite in positive active material of experimental cells after formation and after 6 months. $D[001] = 28.8$ Å.

Fig. 11. A grain of graphite in positive active material of experimental cell after 6 months of float operation.

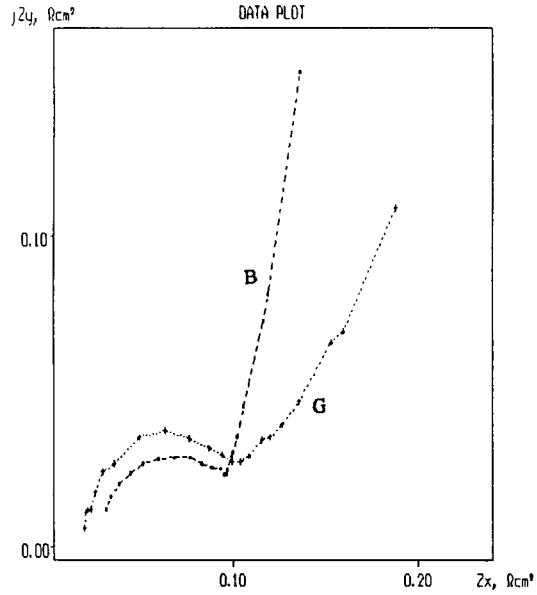

Fig. 12. Impedance diagram of experimental cells: G, 'good' cell, with no PCL; B, 'bad' cells, with PCL.

passivation occurs mainly in the active material, particularly at the electrolyte/active-material interface. Passivation during constant-voltage charging is called CVC-PCL [13]. The addition of graphite reduces premature capacity loss and helps to recover capacity during 'reactivation', but these effects are not very strong. After dismantling cells with paste 3, it was found out that the active material was weakly bonded, i.e., it was very brittle. This is probably due to intercalation of sulfate ions in the graphite grains with subsequent expansion of the grains. During investigation of the phase composition of the active material by XRD, attention was paid to the basic diffraction line $D[001]$ of the graphite that was added to paste 3. Analysis of grain morphology with respect to the presence and the shape of the graphite grains was made using scanning electron microscope. Active material before and immediately after formation revealed the very distinct diffraction line of graphite. During further testing, after different stages of float operation, the graphite diffraction line was not visible. To determine conclusively the behaviour of graphite during battery operation, active material from the positive plates was subjected to chemical treatment. The latter consisted of dissolution of lead compounds by a mixture of hydrazine dihydrochloride, ammonium acetate, and acetic acid. The

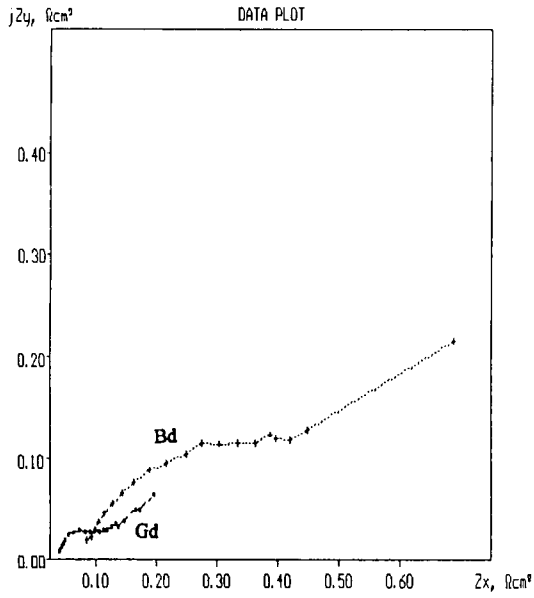

Fig. 13. Impedance diagram of discharged experimental cells: Gd, 'good' discharged cell, with no PCL; Bd, 'bad' discharged cell, with PCL.

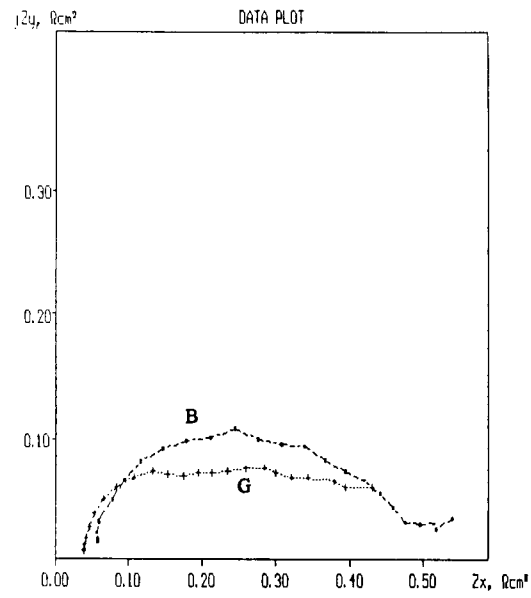

Fig. 15. Impedance diagram of negative plates of experimental cells: G, from a 'good' cell, with no PCL; B, from a 'bad' cell, with PCL.

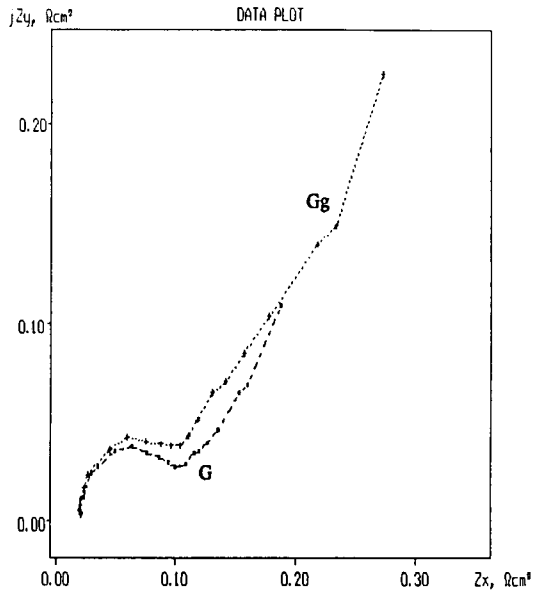

Fig. 14. Impedance diagram of experimental cells: G, 'good' cell, with no PCL; Gg, 'good' cell, with no PCL and with graphite in positive active material.

remaining insoluble part was subjected to phase analysis. It was found out that the graphite was intercalated, and this changes the shape of the diffraction line.

Fig. 10 shows the graphite diffraction line $D[001]$ in positive active material after formation (narrow line) and after 6 months of float operation (broad line). There is not only a considerable broadening of the line, but also a shift in the peak. The latter indicates a change in the lattice constant value from 6.72 to 7.02 Å. The size of the graphite crystallites after intercalation, as calculated from the linewidth by the Hall method, is 28.8 Å, while the size of the initial graphite crystallites was greater than 1000 Å. A photograph of a typical graphite grain is given in Fig. 11. The features support the conclusions obtained from XRD analysis.

An investigation has also been made of the impedance spectra of the test cells. It is found that the transition resistance R_t changes with the state-of-charge (SOC). The influence of cell SOC on impedance spectra has been reported elsewhere [14,15]. Fig. 12 presents the impedance spectra of a 'good' cell (with no PCL) and a 'bad' one (with PCL). The spectra differ one from another, especially at low frequencies. Even greater differences are observed for the same cells in the discharged state (Fig. 13). These differences correspond to R_t values of 0.34 Ω cm^2 for a 'bad' cell and 0.096 Ω cm^2 (i.e., about four times less) for a 'good' one. The impedance spectra of charged cells, with and without graphite in the positive paste, are very similar (Fig. 14); the values are consistent within experimental error. The same is true for discharged cells. This is due to the fact that the impedance spectra of cells are determined mainly by the negative plates.

The impedance spectra taken between two negative plates of a 'good' cell and a 'bad' one are given in Fig. 15. (The cells were open and filled with electrolyte and the positive plates were removed.) The 'bad' battery reveals less flattening of the semicircle and a higher resistance R_s, i.e., the resistance of the electrolyte and the collector. This suggests a change in the porous structure of the plate that results in an inhibition of electrolyte movement into the plate. Impedance spectra of the cells show that the value of R_s in the real component is changed, i.e., it is higher in the discharged

state due to the change of both electrolyte concentration and pore distribution in the plates.

4. Conclusions

Valve-regulated lead/acid batteries with Pb–Ca–Sn grids are susceptible to premature capacity loss (PCL) during float operation. Active materials obtained from tetrabasic lead sulfate (4BS) undergo PCL much more than those obtained from tribasic lead sulfate. Capacity loss can be recovered, at least partially, by constant-current cycling. During the cycling operation, the β-PbO_2 content of the active material increases at the expense of α-PbO_2 content. The addition of graphite to the active material obtained from 4BS reduces PCL and helps to regain capacity during 'reactivation'. Graphite added to the active material undergoes intercalation during battery operation which results in a change in the grain size. Batteries that experience PCL reveal certain differences in impedance spectra as compared with 'good' batteries, both in a charged and a discharged condition. These differences are associated with the charge-transfer resistance and the series resistance, and indicate that the porous structure of the active materials has been changed.

Acknowledgement

This work was sponsored by the State Committee for Scientific Research, Republic of Poland, Project No. 8.0303.91.01.

References

[1] R.V. Biagetti and M.C. Weeks, *The Bell System Tech. J.*, (Sept.) (1970) 1305.

[2] A.C. Simon and S.M. Caulder, in D.H. Collins (ed.), *Power Sources 5, Proc. 9th Int. Power Sources Symp., Brighton, 1974*, Academic Press, London, 1975, Paper No. 7A.

[3] A. Tokunaga, M. Tsubota, K. Yonezu and K. Ando, *J. Electrochem. Soc., 134* (1987) 525.

[4] K. Takahashi, *New Mater. Processes, 3* (1985) 255.

[5] A. Tokunaga, M. Tsubota and K. Yonezu, *J. Electrochem. Soc., 136* (1989) 33.

[6] S.V. Baker, P.T. Moseley and A.D. Turner, *J. Power Sources, 27* (1989) 127.

[7] P. Ruetschi, *J. Electrochem. Soc., 139* (1992) 1347.

[8] J. Kwaśnik, J.D. Milewski, T. Pukacka and B. Szcześniak, *J. Power Sources, 42* (1993) 165.

[9] J. Kwaśnik, J.D. Milewski, T. Pukacka and B. Szcześniak, *Prog. Batt. Batt. Mater., 13* (1994) 219.

[10] J. Kwaśnik, J.D. Milewski, T. Pukacka and B. Szcześniak, *LABAT 93, Varna, Bulgaria, 1993.*

[11] L. Apăteanu, A.F. Hollenkamp and M.J. Koop, *J. Power Sources, 46* (1993) 239.

[12] A. Winsel, E. Voss and U. Hullmeine, *J. Power Sources, 30* (1990) 209.

[13] H. Dietz, H. Niepraschk, K. Wiesener, J. Garche and J. Bauer, *J. Power Sources, 46* (1993) 191.

[14] M. Hughes, R.T. Barton, S.A.G.R. Kartunathilaka and N.A. Hampson, *J. Power Sources, 17* (1986) 305.

[15] A.A. Taganova, I. Mrha, I. Jindra and M. Musilova, *Chimičeskie Istočniki Toka, Sb. Nauchn. Trudov NIAI,* Energoatomizdat, Sankt-Petersburg, 1993, p. 117.